Supplementary content for:
Use of orbitrap−MS/MS and QSAR analyses to estimate mutagenic transformation products of iopamidol generated during ozonation and chlorination

Taku Matsushita[1*], Masahiro Hashizuka[2], Taisuke Kuriyama[2], Yoshihiko Matsui[1] and Nobutaka Shirasaki[1]

[1]Faculty of Engineering, Hokkaido University, N13W8, Sapporo 060-8628, Japan

[2]Graduate School of Engineering, Hokkaido University, N13W8, Sapporo 060-8628, Japan

[*]Corresponding author: taku-m@eng.hokudai.ac.jp; +81−11−706−7279.

Detailed information regarding LC/MS and GC/MS analyses

Iopamidol was quantified by using a hybrid quadrupole-orbitrap mass spectrometer (MS; Q Exactive, Thermo Fisher Scientific Inc., Waltham, MA, USA) coupled with liquid chromatography (LC; UltiMate 3000 LC systems, Thermo Fischer Scientific Inc.). Ten microliters of the sample solution was subjected to the LC. Analysis was performed using a 100 mm × 2.1 mm column with 1.8 μm particle size (Acquity UPLC HSS T3, Waters Corporation, Milford, MA, USA). A binary gradient consisting of (A) 0.05% (v/v) of formic acid in Milli-Q water and (B) 100% methanol at a flow rate of 200 μL/min was used. The gradient program for the mobile phase was as follows: mobile phase (A): mobile phase (B) at 90:10 (v/v) for 0.3 min, increasingly linearly up to 95% mobile phase (B) over a period of 7 min, and then held at the same ratio for another 3 min. MS analysis was performed with an electrospray ionization with 3.5 kV of spray voltage. The temperatures of the capillary and the HESI probe heater were 240 and 450 ºC, respectively. The flow rate of the sheath gas, the auxiliary gas and the sweep gas were 40, 10 and 0 units, respectively. The S-lens ratio frequency level was set at 80. The quantification of iopamidol was conducted in targeted selected ion monitoring (t-SIM) mode with resolution of 70,000 under positive ion mode; the detected fragment ion occurred at *m*/*z* 777.8614.

Accurate masses of transformed products (TPs) were obtained by LC/MS analysis basically in the same LC and MS procedures as iopamidol quantification. The difference was in the operation mode: the accurate masses were obtained in full scan (Full MS) mode (*m*/*z* 200−1000 and 1000−2000) with resolution of 70,000 or 140,000 under both positive and negative ion modes. MS/MS spectra of the TPs were obtained basically in the same LC and MS procedures as iopamidol quantification. The difference was in the operation mode: the spectra were obtained in targeted MS/MS (t-MS^2) mode (collision energy 10, 20 and 30 eV; isolation window 0.4 *m*/*z*) with resolution of 70,000 under suitable ion mode (positive or negative) for each TP.

Iodoacetic acid was quantified by using a hybrid quadrupole-orbitrap MS (Q Exactive) coupled with LC (UltiMate 3000 LC systems). Ten microliters of the sample solution was subjected to the LC. Analysis was performed using a 150 mm × 4.6 mm column with 5 μm particle size (Zorbax C8, Agilent Technologies, Palo Alto, CA, USA). The mobile phase was 0.1% acetic acid in Milli-Q

water and 100% acetonitrile (40:60, v:v), and the flow rate was 200 μL/min. MS analysis was performed with an electrospray ionization with −2.5 kV of spray voltage. The temperatures of the capillary and the HESI probe heater were 250 and 400 ºC, respectively. The flow rate of the sheath gas, the auxiliary gas and the sweep gas were 45, 10 and 2 units, respectively. The S-lens ratio frequency level was set at 50. The quantification of iodoacetic acid was conducted in t-MS^2 mode with resolution of 70,000 under negative ion mode; the detected fragment ion occurred at *m*/*z* 184.9105 → 126.9050 with collision energy of 30 eV.

Iodoform was quantified by using a GC/MS system (QP2010 Plus, Shimadzu Corporation, Kyoto, Japan) equipped with a capillary column (DB-1ms UI, Agilent Technologies; length, 30 m; internal diameter, 0.25 mm; thickness, 0.25 μm). Injection volume was 2.5 μL. The temperature of the ion source, injector and transfer line was 280 ºC. The column temperature was programmed in isothermal runs at 30 ºC for 10 min, at a rate of 6 ºC/min up to 45 ºC, at a rate of 36 ºC/min up to 280 ºC, and then held at 280 ºC for 5 min. GC/MS analysis was performed in SIM mode with 1,2-dibromopropane as an internal standard; the detected fragment ions of iodoform and 1,2-dibromopropane occurred at *m*/*z* 394 and 121, respectively.

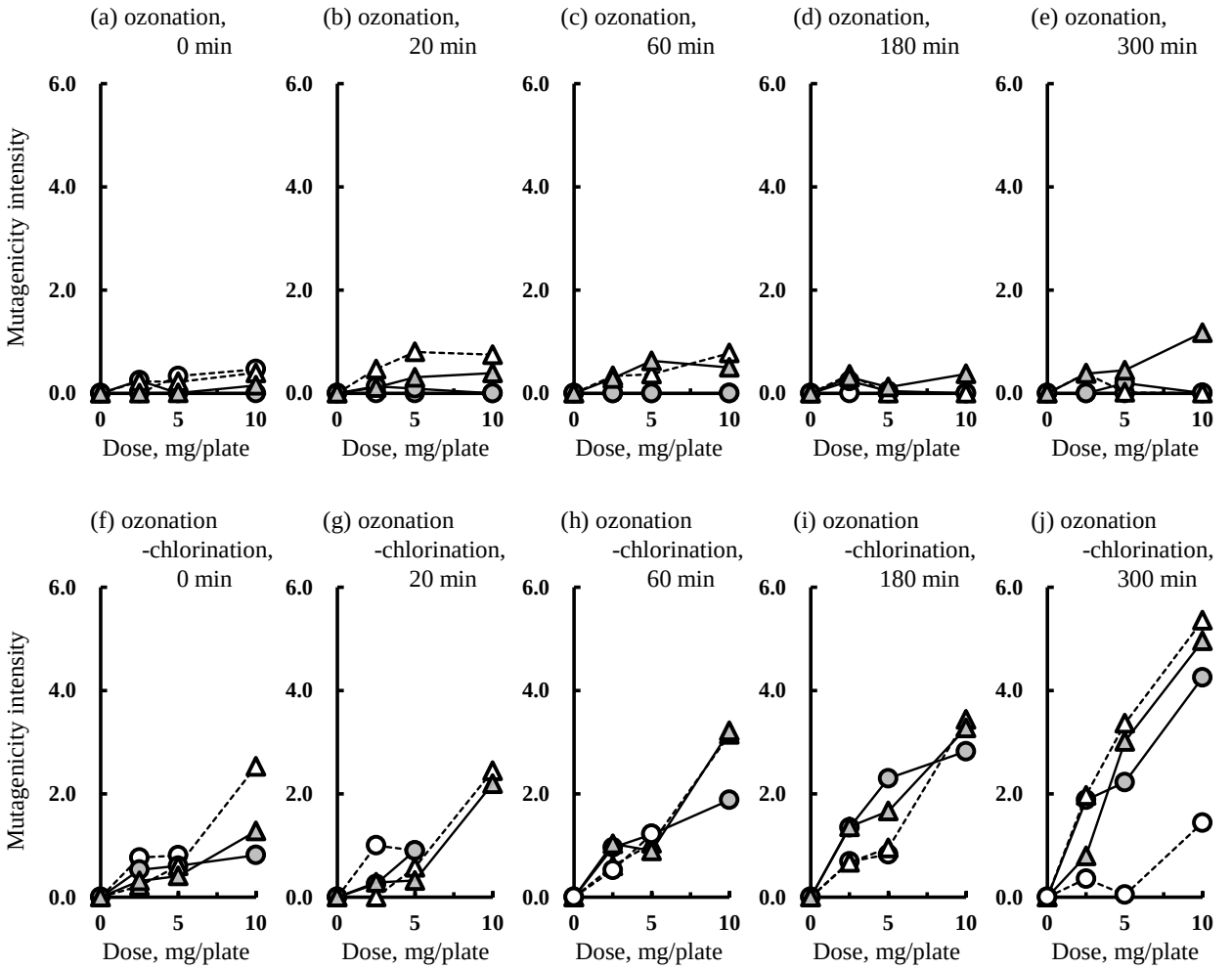

Fig. S1 Dose-response curves of Ames assay conducted on samples treated with ozonation (a-e) and ozonation-chlorination (f-j). Dose in x-axis shows the initial amount of iopamidol that had been contained in the samples before ozonation. White circles, TA98 without metabolic activation; gray circles, TA98 with metabolic activation; white triangles, TA100 without metabolic activation; and gray triangles, TA100 with metabolic activation.

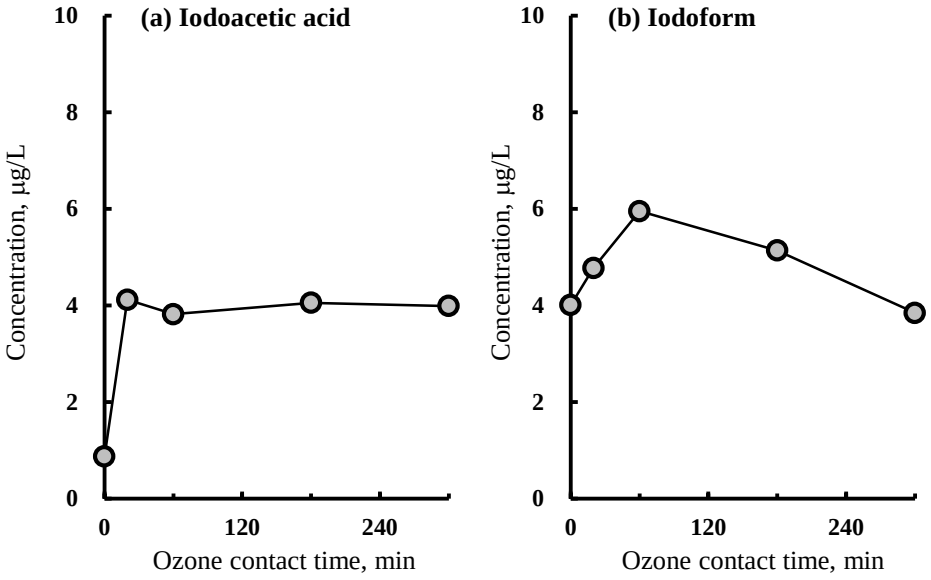

Fig. S2 Changes in the concentration of iodoacetic acid (a) and iodoform (b) with ozonation time during the ozonation–chlorination process.

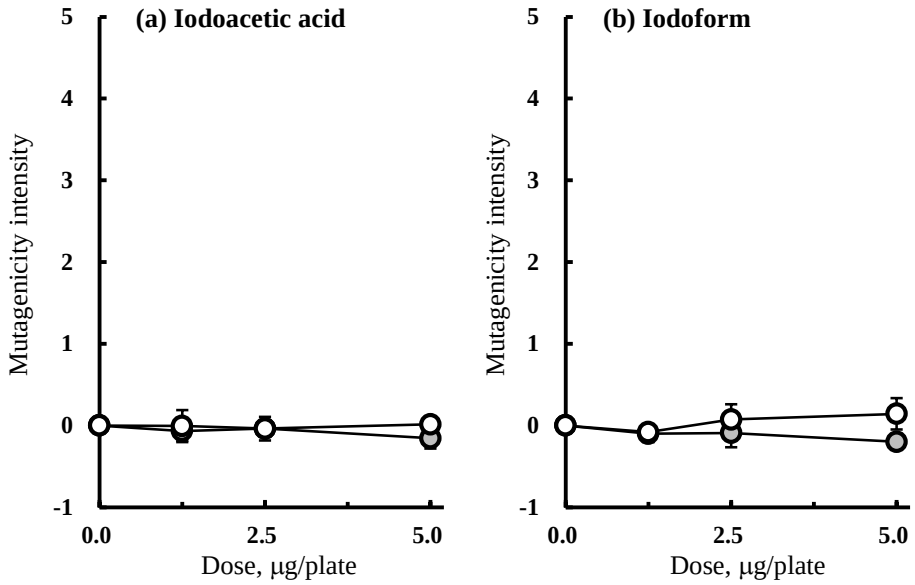

Fig. S3 Mutagenicity induced by iodoacetic acid (a) and iodoform (b) in TA100 as assessed by using the Ames assay. Gray and white circles indicate data from experiments conducted with and without S9 mix, respectively. Error bars indicate SDs of four plates. Mutagenicity is expressed as "mutagenicity intensity", which is defined as the ratio of the number of net His^+ revertants per plate to the number of spontaneous revertants per plate.

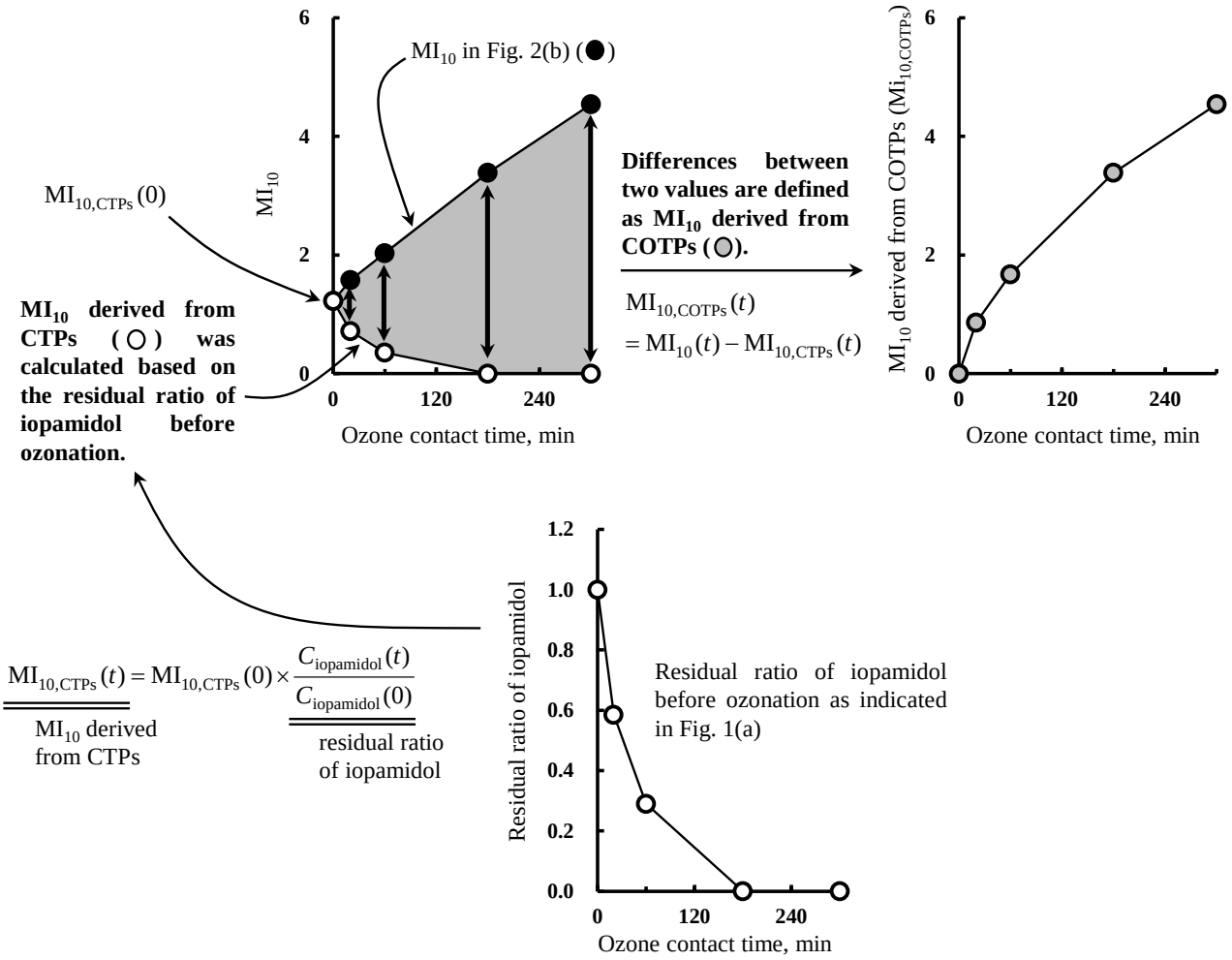

Fig. S4 Procedures for calculating MI_{10} derived from COTPs from the observed MI_{10} and the residual ratio of iopamidol.

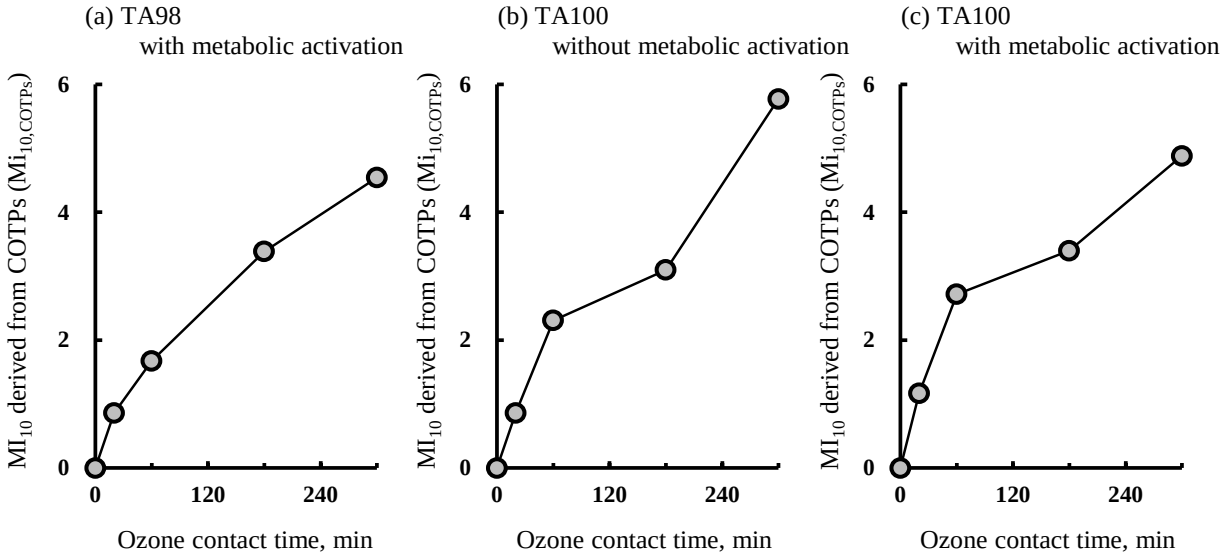

Fig. S5 Changes in mutagenicity derived from COTPs with ozone contact time during the ozonation−chlorination process. Mutagenicity is expressed as "MI_{10}", which is defined as mutagenicity intensity (i.e., the ratio of the number of net His^+ revertants per plate to the number of spontaneous revertants per plate) at the dose of sample solution that had initially contained 10 mg of iopamidol before ozonation. The MI_{10} values were modified by using the iopamidol concentration remaining before chlorination under the assumption that the extent of total mutagenicity induced by the reported chlorination-TPs was proportional to the iopamidol concentration remaining before chlorination.

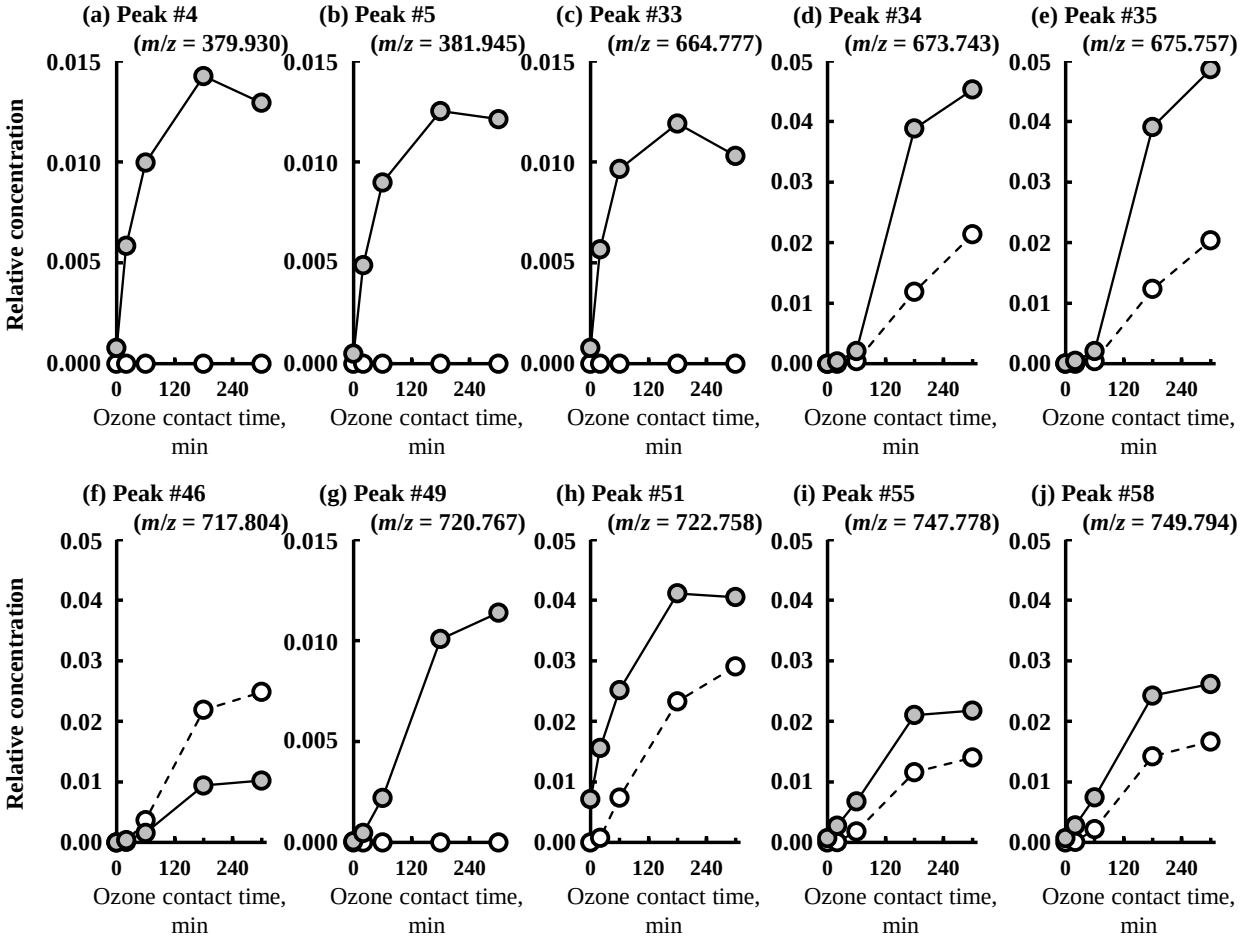

Fig. S6 Comparison of the peak areas that were positively correlated with the observed mutagenicity between the ozonation (white circles) and the ozonation−chlorination (gray circles) process.

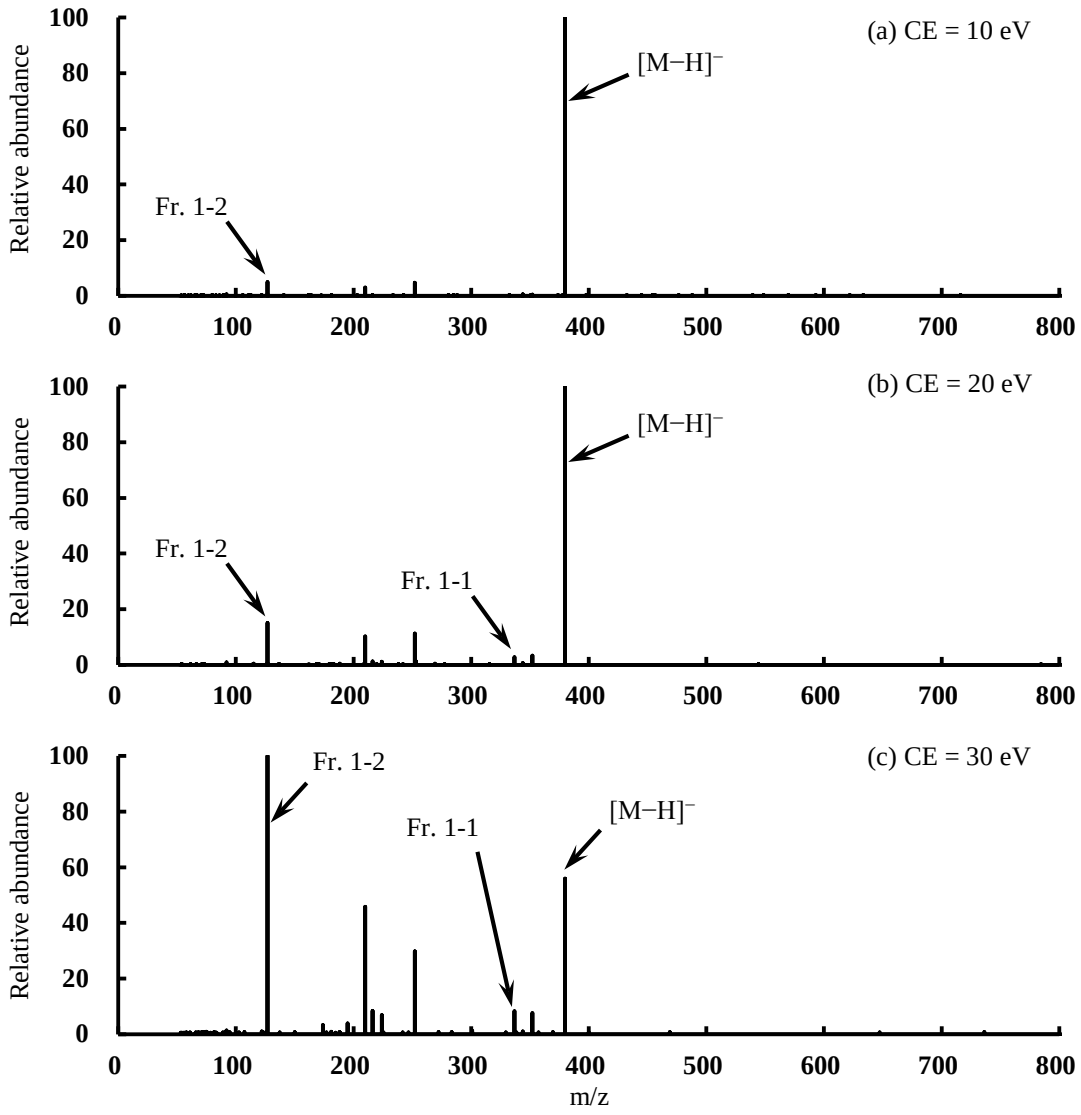

Fig. S7 MS/MS spectra of Peak #4 (*m*/*z* = 379.930, negative ion mode) with different values of collision energy (CE). Fragment numbers (Frs. 1-1 and -2) are corresponding to the structures indicated as the same numbers in Fig. S8.

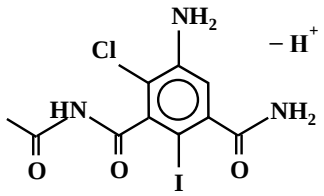

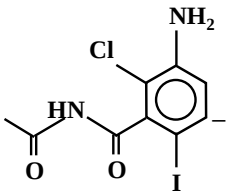

I^-

Precursor ion ($C_{10}H_8O_3N_3ClI$)		**Fr. 1-1** ($C_9H_7O_2N_2ClI$)		**Fr. 1-2** (I)	
Theoretical *m*/*z*	379.9304	Theoretical *m*/*z*	336.9246	Theoretical *m*/*z*	126.9039
10 eV	379.9307	10 eV	N.D.	10 eV	126.9044
20 eV	379.9309	20 eV	336.9251	20 eV	126.9045
30 eV	379.9308	30 eV	336.9248	30 eV	126.9045
50 eV	379.9306	50 eV	N.D.	50 eV	126.9044

Fig. S8 Attributes of the fragments observed after MS/MS analysis of Peak #4 (*m*/*z* = 379.930, negative ion mode). Fragment numbers (Frs. 1-1 and 1-2) are corresponding to the fragment ions assigned as the same numbers in Fig. S7.

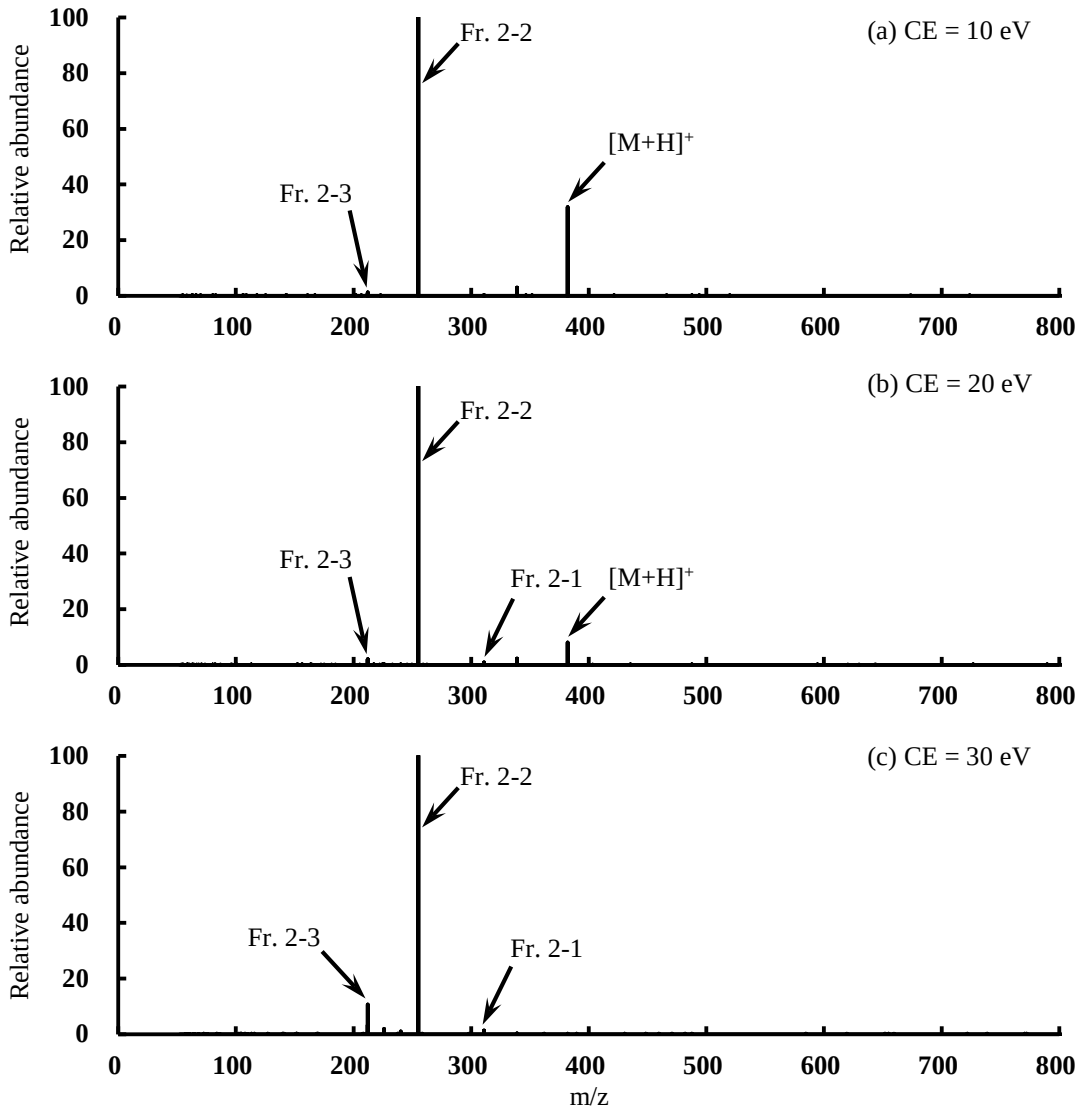

Fig. S9 MS/MS spectra of Peak #5 (m/z = 381.945, positive ion mode) with different values of collision energy (CE). Fragment numbers (Frs. 2-1−3) are corresponding to the structures indicated as the same numbers in Fig. S10.

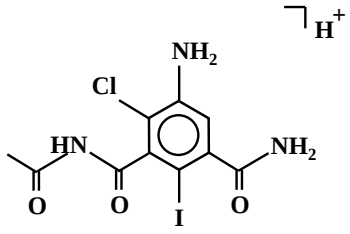

Precursor ion ($C_{10}H_{10}O_3N_3ClI$)

Theoretical *m*/*z*	381.9450
10 eV	381.9452
20 eV	381.9452
30 eV	381.9454
50 eV	N.D.

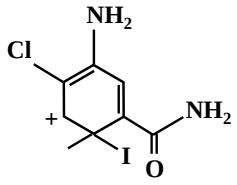

Fr. 2-1 ($C_8H_9ON_2ClI$)

Theoretical *m*/*z*	310.9443
10 eV	310.9446
20 eV	310.9445
30 eV	310.9446
50 eV	310.9446

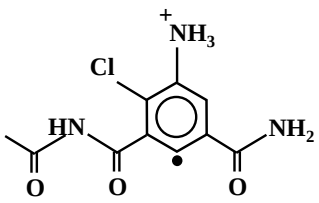

Fr. 2-2 ($C_{10}H_{10}O_3N_3Cl$)

Theoretical *m*/*z*	255.0405
10 eV	255.0407
20 eV	255.0407
30 eV	255.0407
50 eV	255.0407

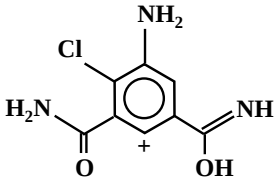

Fr. 2-3 ($C_8H_7O_2N_3Cl$)

Theoretical *m*/*z*	212.0221
10 eV	212.0221
20 eV	212.0221
30 eV	212.0222
50 eV	212.0222

Fig. S10 Attributes of the fragments observed after MS/MS analysis of Peak #5 (*m*/*z* = 381.945, positive ion mode). Fragment numbers (Frs. 2-1−3) are corresponding to the fragment ions assigned as the same numbers in Fig. S9.

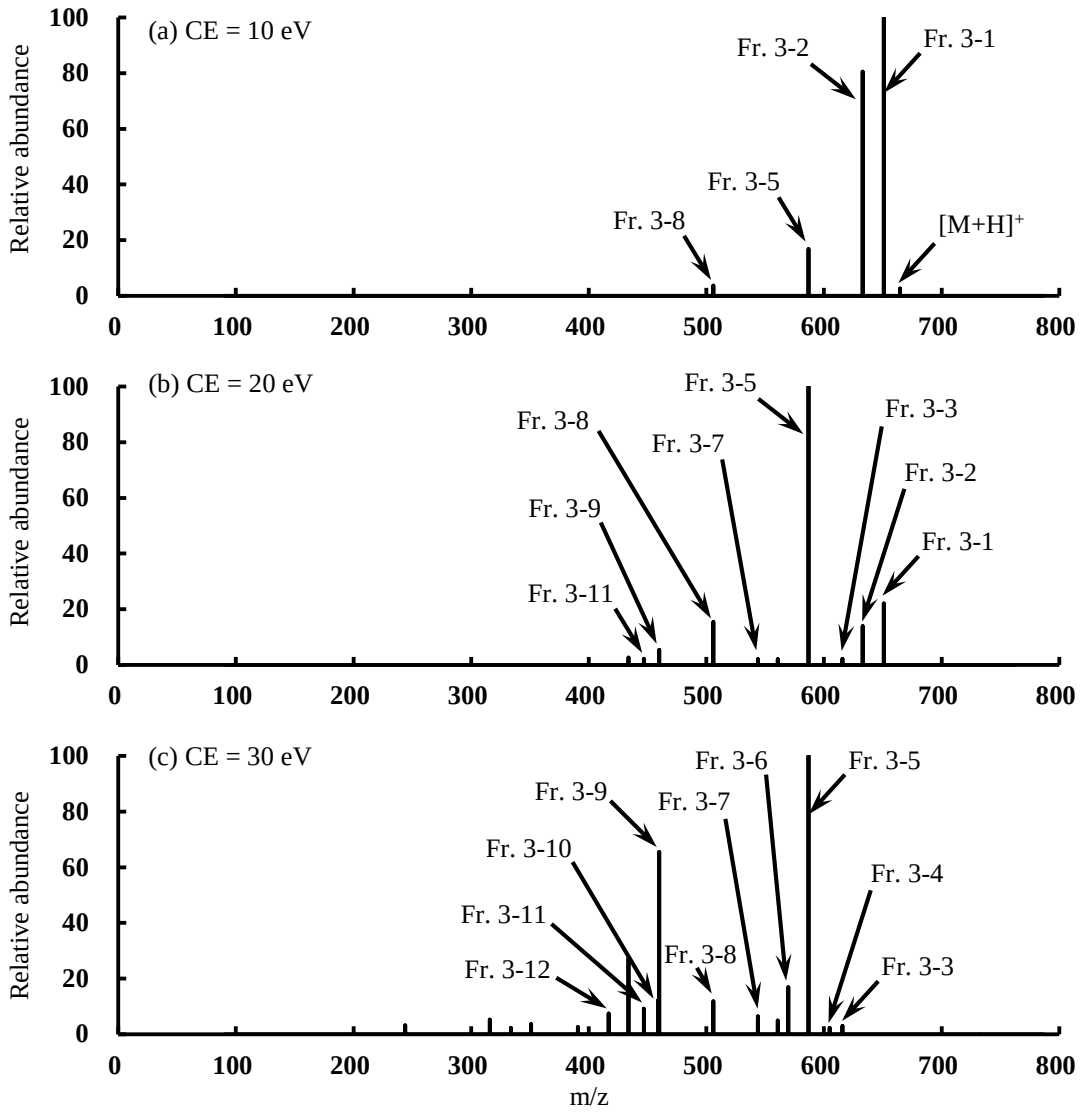

Fig. S11 MS/MS spectra of Peak #33 (m/z = 664.777, positive ion mode) with different values of collision energy (CE). Fragment numbers (Frs. 3-1−12) are corresponding to the structures indicated as the same numbers in Fig. S12.

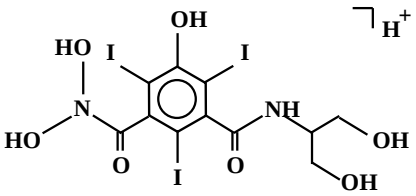

Precursor ion ($C_{11}H_{12}O_7N_2I_3$)

Theoretical *m/z*	664.7773
10 eV	664.7791
20 eV	664.7785
30 eV	N.D.
50 eV	N.D.

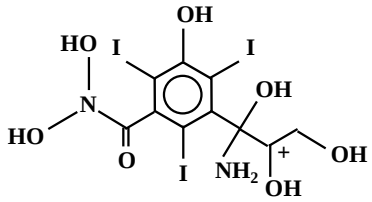

Fr. 3-1 ($C_{10}H_{10}O_7N_2I_3$)

Theoretical *m/z*	650.7617
10 eV	650.7639
20 eV	650.7635
30 eV	650.7639
50 eV	N.D.

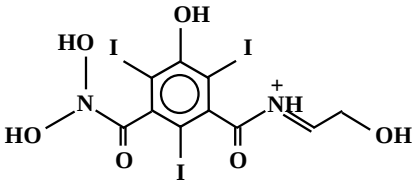

Fr. 3-2 ($C_{10}H_8O_6N_2I_3$)

Theoretical *m/z*	632.7511
10 eV	632.7515
20 eV	632.7511
30 eV	632.7513
50 eV	N.D.

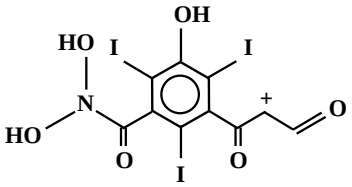

Fr. 3-3 ($C_{10}H_5O_6NI_3$)

Theoretical *m/z*	615.7245
10 eV	615.7262
20 eV	615.7257
30 eV	615.7263
50 eV	N.D.

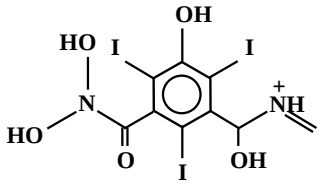

Fr. 3-4 ($C_9H_8O_5N_2I_3$)

Theoretical *m/z*	604.7562
10 eV	N.D.
20 eV	604.7570
30 eV	604.7577
50 eV	N.D.

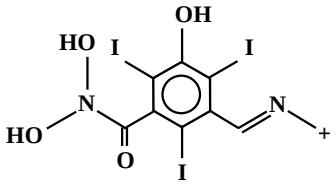

Fr. 3-5 ($C_9H_6O_4N_2I_3$)

Theoretical *m/z*	586.7456
10 eV	586.7468
20 eV	586.7464
30 eV	586.7468
50 eV	N.D.

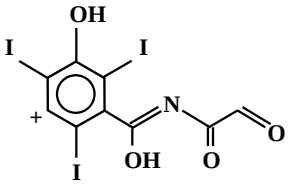

Fr. 3-6 ($C_9H_3O_4NI_3$)

Theoretical *m/z*	569.7191
10 eV	N.D.
20 eV	569.7188
30 eV	569.7193
50 eV	N.D.

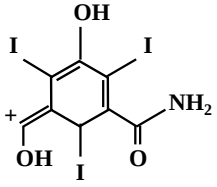

Fr. 3-7 ($C_8H_5O_3NI_3$)

Theoretical *m/z*	543.7398
10 eV	543.7406
20 eV	543.7406
30 eV	543.7407
50 eV	N.D.

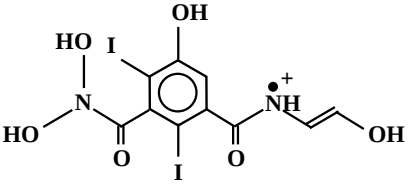

Fr. 3-8 ($C_{10}H_8O_6N_2I_2$)

Theoretical *m/z*	505.8466
10 eV	505.8479
20 eV	505.8476
30 eV	505.8479
50 eV	N.D.

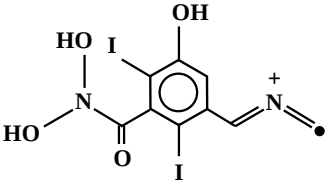

Fr. 3-9 ($C_9H_6O_4N_2I_2$)

Theoretical *m/z*	459.8411
10 eV	459.8424
20 eV	459.8420
30 eV	459.8423
50 eV	N.D.

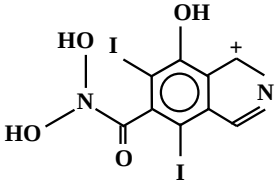

Fr. 3-10 ($C_9H_5O_4N_2I_2$)

Theoretical *m/z*	458.8333
10 eV	N.D.
20 eV	458.8336
30 eV	458.8338
50 eV	N.D.

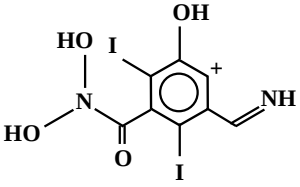

Fr. 3-11 ($C_8H_5O_4N_2I_2$)

Theoretical *m/z*	446.8333
10 eV	N.D.
20 eV	456.8336
30 eV	456.8339
50 eV	N.D.

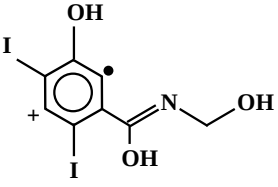

Fr. 3-12 ($C_8H_5O_3NI_2$)

Theoretical *m/z*	416.8353
10 eV	N.D.
20 eV	416.8355
30 eV	416.8356
50 eV	N.D.

Fig. S12 Attributes of the fragments observed after MS/MS analysis of Peak #33 (*m/z* = 664.777, positive ion mode). Fragment numbers (Frs. 3-1−12) are corresponding to the fragment ions assigned as the same numbers in Fig. S11.

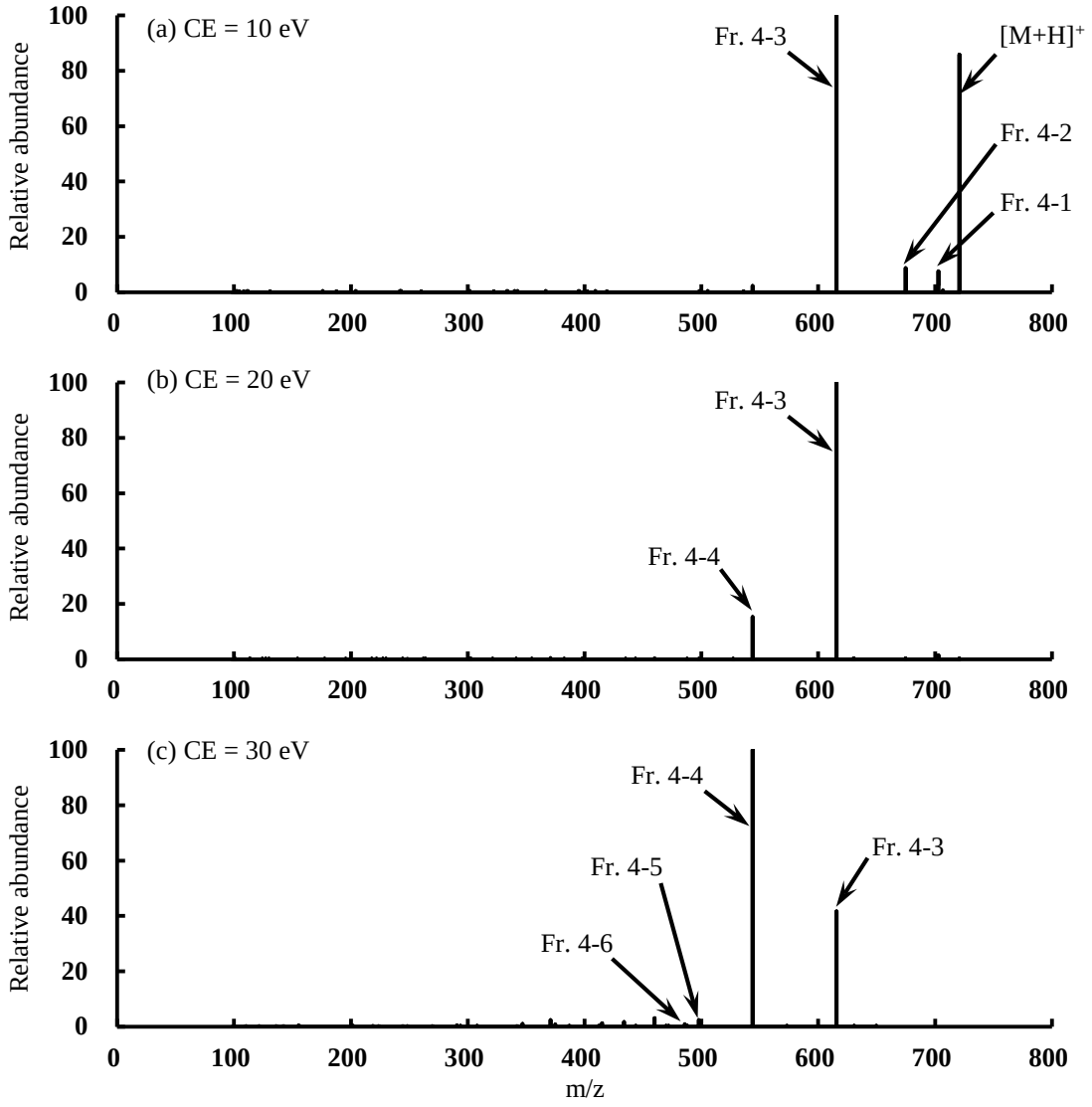

Fig. S13 MS/MS spectra of Peak #49 (*m*/*z* = 720.767, positive ion mode) with different values of collision energy (CE). Fragment numbers (Frs. 4-1−6) are corresponding to the structures indicated as the same numbers in Fig. S14.

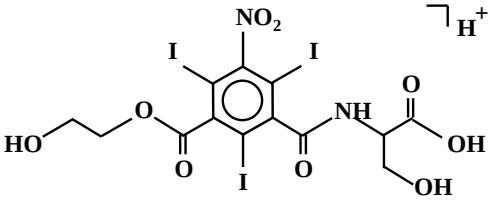

Precursor ion ($C_{13}H_{12}O_9N_2I_3$)

Theoretical *m*/*z*	720.7671
10 eV	720.7669
20 eV	720.7670
30 eV	N.D.

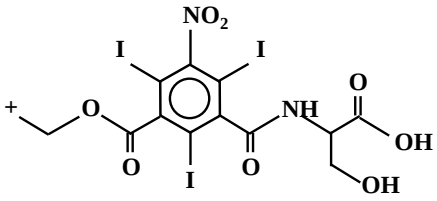

Fr. 4-1 ($C_{13}H_{10}O_8N_2I_3$)

Theoretical *m*/*z*	702.7566
10 eV	702.7570
20 eV	702.7556
30 eV	N.D.

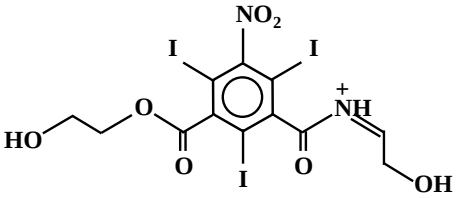

Fr. 4-2 ($C_{12}H_{10}O_7N_2I_3$)

Theoretical *m*/*z*	674.7617
10 eV	674.7612
20 eV	674.7616
30 eV	N.D.

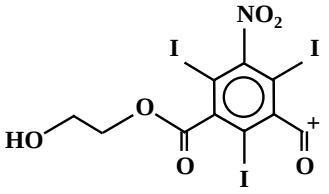

Fr. 4-3 ($C_{10}H_5O_6NI_3$)

Theoretical *m*/*z*	615.7245
10 eV	615.7242
20 eV	615.7241
30 eV	615.7241

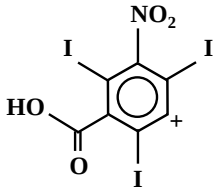

Fr. 4-4 ($C_7HO_4NI_3$)

Theoretical *m*/*z*	543.7034
10 eV	543.7032
20 eV	543.7035
30 eV	543.7034

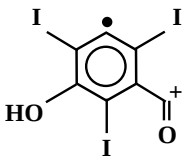

Fr. 4-5 ($C_7HO_2I_3$)

Theoretical *m*/*z*	497.7105
10 eV	N.D.
20 eV	497.7109
30 eV	497.7100

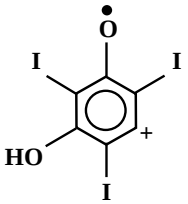

Fr. 4-6 ($C_6HO_2I_3$)

Theoretical *m*/*z*	485.7105
10 eV	N.D.
20 eV	N.D.
30 eV	485.7106

Fig. S14 Attributes of the fragments observed after MS/MS analysis of Peak #49 (*m*/*z* = 720.767, positive ion mode). Fragment numbers (Frs. 4-1−6) are corresponding to the fragment ions assigned as the same numbers in Fig. S13.

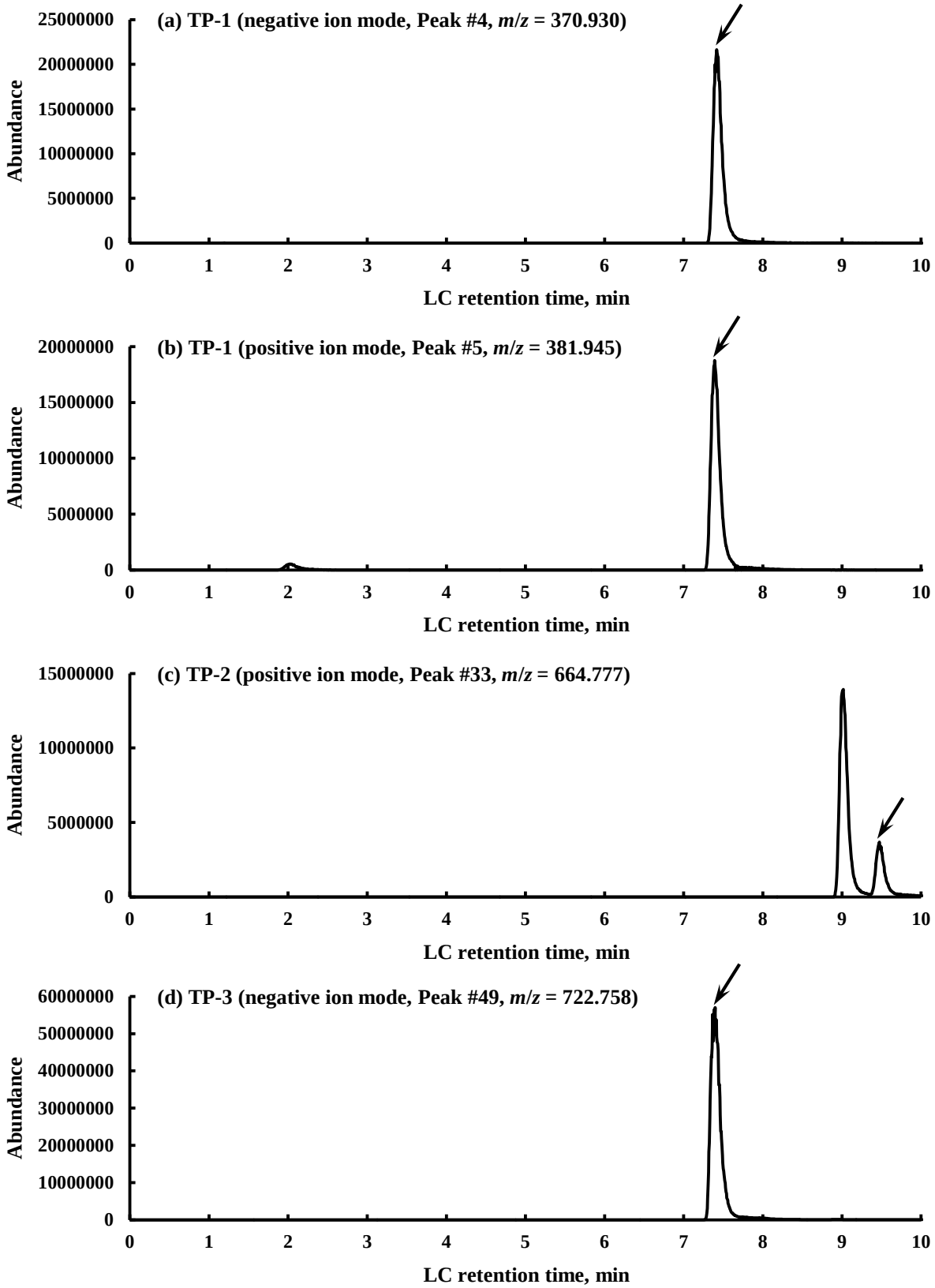

Fig. S15 LC/MS chromatograms of TPs thought to contribute to the observed mutagenicity. Arrows indicate corresponding peaks.

Table S1 Coefficients of determination between the relative concentrations of the detected transformation products and the mutagenicity intensity (MI_{10}). The regression lines were calculated to pass through the origin. Transformation products with $r^2 \geq 0.6$ are highlighted in gray.

#	m/z	Retention time, min	Ion mode	Maximum relative concentration	Coefficient of determination (r^2) TA98 +S9 mix	TA100 -S9 mix	TA100 +S9 mix
1	362.032	7.76	n	0.03	-2.20	-2.72	-2.02
2	362.032	6.67	n	0.03	-2.20	-2.72	-2.02
3	364.919	7.42	p	0.06	-0.68	-0.97	-0.39
4	**379.930**	**7.42**	**n**	**0.01**	**0.64**	0.08	**0.71**
5	**381.945**	**7.42**	**p**	**0.01**	**0.67**	0.14	**0.74**
6	400.023	2.86	p	0.01	-1.56	-1.94	-1.30
7	453.967	7.18	n	0.09	-1.74	-2.19	-1.47
8	455.982	7.17	p	0.08	-1.21	-1.58	-0.96
9	477.907	7.73	p	0.03	-1.94	-2.19	-1.87
10	520.903	9.29	n	0.01	-2.35	-2.90	-2.15
11	520.962	1.55	p	0.01	-3.09	-3.62	-3.29
12	521.898	7.73	n	0.02	-2.31	-2.69	-2.29
13	522.917	9.23	p	0.03	-2.18	-2.69	-1.95
14	536.933	9.82	p	0.02	-3.19	-3.99	-3.22
15	538.888	7.73	n	0.02	-2.16	-2.49	-2.12
16	540.885	7.73	n	0.01	-2.19	-2.53	-2.15
17	569.842	7.60	p	0.06	-1.07	-1.29	-0.83
18	577.882	6.66	n	0.09	-3.38	-4.07	-3.67
19	579.896	6.75	p	0.12	-3.32	-3.97	-3.58
20	612.838	9.19	n	0.05	-2.50	-3.08	-2.36
21	612.897	1.55	p	0.01	-3.13	-3.66	-3.40
22	613.833	7.63	n	0.03	-1.42	-1.69	-1.23
23	614.853	9.17	p	0.09	-2.29	-2.81	-2.08
24	630.823	7.63	n	0.02	-0.38	-0.58	-0.19
25	641.778	7.17	n	0.24	-3.35	-3.98	-3.65
26	643.881	7.37	p	0.13	-3.16	-3.70	-3.39
27	650.935	5.61	n	0.02	-3.36	-4.04	-3.61
28	656.876	1.56	n	0.02	-3.21	-3.77	-3.49
29	658.890	1.55	p	0.01	-3.13	-3.65	-3.39
30	659.763	7.40	n	0.04	-0.31	-0.54	-0.08
31	659.789	4.21	n	0.07	-3.36	-4.02	-3.64
32	661.778	7.38	p	0.17	-0.12	-0.33	0.12
33	**664.777**	**9.46**	**p**	**0.01**	0.50	-0.02	**0.65**
34	673.743	7.50	n	0.05	0.03	-0.96	-0.48
35	675.757	7.34	p	0.05	0.05	-0.90	-0.46
36	687.870	7.38	n	0.14	-3.19	-3.76	-3.43
37	701.811	1.86	n	0.05	-1.92	-2.40	-1.72
38	703.825	1.86	p	0.09	-1.90	-2.74	-2.33
39	704.774	8.91	n	0.12	-2.48	-3.04	-2.35
40	704.809	2.11	n	0.04	-3.43	-4.06	-3.76
41	704.832	1.55	p	0.01	-3.26	-3.83	-3.58
42	705.768	7.40	n	0.11	-0.25	-0.49	-0.02
43	705.793	3.97	p	0.30	-3.30	-3.91	-3.55
44	706.788	8.90	p	0.18	-2.28	-2.78	-2.10
45	706.825	2.10	p	0.06	-3.49	-4.15	-3.86
46	717.804	2.13	p	0.01	0.24	-0.70	-0.18
47	718.824	7.67	p	0.03	-3.33	-3.93	-3.63
48	719.808	7.17	p	0.41	-3.25	-3.84	-3.49
49	720.767	9.06	p	0.01	0.34	-0.54	-0.04
50	720.803	9.40	p	0.07	-3.26	-4.06	-3.29
51	**722.758**	**7.40**	**n**	**0.04**	**0.85**	0.38	**0.82**
52	733.801	7.89	n	0.01	-3.28	-3.86	-3.60
53	734.855	7.80	p	0.01	-3.31	-3.92	-3.57
54	735.815	7.24	p	0.32	-2.94	-3.42	-3.15
55	747.778	7.40	n	0.02	0.56	-0.25	0.28
56	747.816	1.86	n	0.02	-1.98	-2.45	-1.76
57	748.812	1.56	n	0.03	-3.27	-3.85	-3.58
58	749.794	7.31	p	0.03	0.54	-0.26	0.24
59	776.831	5.99	n	0.81	-3.34	-3.94	-3.64
60	777.815	8.00	n	0.01	-3.33	-3.97	-3.62
61	778.846	6.01	p	1.51	-3.38	-4.02	-3.71
62	779.806	7.23	n	0.29	-2.99	-3.48	-3.19
63	779.829	8.00	p	0.03	-3.34	-3.97	-3.63
64	790.810	6.36	n	0.01	0.11	-0.16	0.39
65	792.825	6.36	p	0.02	0.28	0.05	0.56
66	792.861	7.48	p	1.22	-3.48	-4.14	-3.84
67	793.845	8.71	p	0.03	-3.47	-4.16	-3.82
68	796.795	7.23	n	0.08	-2.55	-2.91	-2.62
69	806.840	7.58	p	0.01	-0.43	-0.72	-0.07
70	836.852	7.47	n	0.61	-3.48	-4.14	-3.84

Table S2 Coefficients of determination between the relative concentrations of the detected transformation products and the mutagenicity derived from COTPs ($MI_{10,COTPs}$). The regression lines were calculated to pass through the origin. TPs with $r^2 \geq 0.6$ are highlighted in gray.

#	m/z	Retention time, min	Ion mode	Maximum relative concentration	Coefficient of determination (r^2) TA98 +S9 mix	TA100 -S9 mix	TA100 +S9 mix
1	362.032	7.76	n	0.03	-0.90	-0.81	-0.93
2	362.032	6.67	n	0.03	-0.90	-0.81	-0.93
3	364.919	7.42	p	0.06	-0.15	-0.11	-0.03
4	**379.930**	**7.42**	**n**	**0.01**	**0.80**	**0.69**	**0.85**
5	**381.945**	**7.42**	**p**	**0.01**	**0.83**	**0.74**	**0.89**
6	400.023	2.86	p	0.01	-0.61	-0.54	-0.56
7	453.967	7.18	n	0.09	-0.68	-0.60	-0.63
8	455.982	7.17	p	0.08	-0.44	-0.38	-0.37
9	477.907	7.73	p	0.03	-0.93	-0.83	-1.01
10	520.903	9.29	n	0.01	-0.96	-0.85	-0.99
11	520.962	1.55	p	0.01	-1.40	-1.27	-1.68
12	521.898	7.73	n	0.02	-1.07	-0.96	-1.19
13	522.917	9.23	p	0.03	-0.88	-0.77	-0.88
14	536.933	9.82	p	0.02	-1.31	-1.18	-1.50
15	538.888	7.73	n	0.02	-1.01	-0.91	-1.11
16	540.885	7.73	n	0.01	-1.03	-0.92	-1.13
17	569.842	7.60	p	0.06	-0.44	-0.38	-0.04
18	577.882	6.66	n	0.09	-1.48	-1.35	-1.82
19	579.896	6.75	p	0.12	-1.46	-1.33	-1.79
20	612.838	9.19	n	0.05	-1.04	-0.92	-1.10
21	612.897	1.55	p	0.01	-1.43	-1.29	-1.74
22	613.833	7.63	n	0.03	-0.62	-0.55	-0.60
23	614.853	9.17	p	0.09	-0.94	-0.83	-0.96
24	630.823	7.63	n	0.02	-0.10	-0.09	-0.02
25	641.778	7.17	n	0.24	-1.48	-1.35	-1.83
26	643.881	7.37	p	0.13	-1.43	-1.29	-1.73
27	650.935	5.61	n	0.02	-1.47	-1.33	-1.79
28	656.876	1.56	n	0.02	-1.45	-1.31	-1.77
29	658.890	1.55	p	0.01	-1.42	-1.29	-1.74
30	659.763	7.40	n	0.04	-0.01	-0.01	0.10
31	659.789	4.21	n	0.07	-1.48	-1.34	-1.81
32	661.778	7.38	p	0.17	0.10	0.10	0.22
33	**664.777**	**9.46**	**p**	**0.01**	**0.68**	0.59	**0.78**
34	**673.743**	**7.50**	**n**	**0.05**	**0.78**	**0.65**	0.46
35	**675.757**	**7.34**	**p**	**0.05**	**0.79**	**0.68**	0.47
36	687.870	7.38	n	0.14	-1.43	-1.30	-1.74
37	701.811	1.86	n	0.05	-0.78	-0.70	-0.78
38	703.825	1.86	p	0.09	-0.76	-0.79	-1.07
39	704.774	8.91	n	0.12	-1.04	-0.93	-1.11
40	704.809	2.11	n	0.04	-1.51	-1.37	-1.87
41	704.832	1.55	p	0.01	-1.47	-1.33	-1.81
42	705.768	7.40	n	0.11	0.03	0.03	0.14
43	705.793	3.97	p	0.30	-1.46	-1.33	-1.78
44	706.788	8.90	p	0.18	-0.95	-0.84	-0.99
45	706.825	2.10	p	0.06	-1.52	-1.39	-1.90
46	**717.804**	**2.13**	**p**	**0.01**	**0.86**	**0.72**	**0.60**
47	718.824	7.67	p	0.03	-1.48	-1.34	-1.82
48	719.808	7.17	p	0.41	-1.45	-1.32	-1.76
49	**720.767**	**9.06**	**p**	**0.01**	**0.90**	**0.77**	**0.67**
50	720.803	9.40	p	0.07	-1.33	-1.20	-1.54
51	**722.758**	**7.40**	**n**	**0.04**	**0.86**	**0.75**	**0.87**
52	733.801	7.89	n	0.01	-1.47	-1.34	-1.82
53	734.855	7.80	p	0.01	-1.47	-1.33	-1.79
54	735.815	7.24	p	0.32	-1.36	-1.23	-1.63
55	**747.778**	**7.40**	**n**	**0.02**	**0.94**	**0.80**	**0.78**
56	747.816	1.86	n	0.02	-0.80	-0.71	-0.80
57	748.812	1.56	n	0.03	-1.47	-1.33	-1.81
58	**749.794**	**7.31**	**p**	**0.03**	**0.94**	**0.81**	**0.77**
59	776.831	5.99	n	0.81	-1.48	-1.35	-1.83
60	777.815	8.00	n	0.01	-1.47	-1.34	-1.81
61	778.846	6.01	p	1.51	-1.49	-1.36	-1.85
62	779.806	7.23	n	0.29	-1.37	-1.24	-1.65
63	779.829	8.00	p	0.03	-1.48	-1.35	-1.82
64	790.810	6.36	n	0.01	0.30	0.29	0.45
65	792.825	6.36	p	0.02	0.42	0.41	0.58
66	792.861	7.48	p	1.22	-1.52	-1.38	-1.90
67	793.845	8.71	p	0.03	-1.51	-1.38	-1.88
68	796.795	7.23	n	0.08	-1.21	-1.09	-1.40
69	806.840	7.58	p	0.01	0.02	0.04	0.18
70	836.852	7.47	n	0.61	-1.52	-1.38	-1.90